Genomic architecture of nestmate recognition cues in the desert ant

Pnina Cohen*, Shani Inbar*, Eyal Privman#

Department of Evolutionary and Environmental Biology, Institute of Evolution, University of Haifa, Haifa, Israel

* Equal contribution

Corresponding author

Abstract

Nestmate recognition underlies social behaviour in social insects as it forms the basis for cooperation within the colony. Quantitative variation in cuticle hydrocarbons (CHCs) is used for nestmate recognition in ants and other social insects. We carried out a Genome Wide Association Study (GWAS) of CHCs in the desert ant *Cataglyphis niger* by sampling 47 colonies, fully sequencing six workers from each colony and measuring the relative amounts of their CHCs. Under the Gestalt colony odour model, social interactions between nestmates, in which CHCs are being transferred and mixed, are essential in creating a uniform colony CHCs profile. Therefore, we carried out a second GWAS between the colonies and their uniform Gestalt odour by averaging nestmate genotypes and comparing them to their averaged CHCs amounts. Together, these two analyses identified 99 QTLs associated with 18 of the CHCs. Thirteen clusters of two to four QTLs located within 10cM from each other were identified, seven of which contained QTLs from both analyses. We conclude that nestmate recognition, a quantitative and complex colony-level trait, has a genetic component to its phenotypic variation. Our results are in line with the hypothesis that social interactions between nestmates are an important component of the mechanisms that determine the chemical ID of a colony.

Introduction

Colonial identity makes the foundation for any social interaction in insect societies. The ability to recognize nestmates and to discriminate them from aliens is needed for protecting the colony's food reserves and brood from being plundered and for preserving territorial control over resources around the nest. In addition, it is crucial for the maintenance of genetic integrity of a colony against social parasites, in keeps with Hamilton's principles of kin selection and inclusive fitness[1,2]. The chemical cues which are reportedly involved in nestmate recognition are lipids found on the cuticle[3–7], mainly n-alkanes, methyl-branched, and unsaturated hydrocarbons. Insect cuticular hydrocarbons (CHCs) chains vary in length (up to 60, but mostly between 20 and 40 carbons), number and positions of methyl branches, and number and positions of double bonds[8]. In social insects, the number of different CHCs is especially large[9] and tens of different hydrocarbons may be present on the body surface of a single individual. While different insect species have qualitatively distinct mixtures of CHCs, intraspecific variation of CHCs mixtures is largely quantitative. The relative amounts of each CHC creates an individual's chemical profile and thereby its identity[10–12].

In ants, the number of different CHCs is especially large, even in comparison to other social insects[9]. Intra-colony CHCs composition variability is smaller inter-colony variability[5,13], and some studies reported that chemical distances between colonies correlate with aggression levels between members of these colonies[14–16]. Diet, nest material and other environmental factors were shown to influence ant CHC profiles[17–19]

and thereby affect nestmate recognition and inter-colony aggression. It has been suggested that genetics is also an important contributor to the colony-specific composition of CHCs[14,16,20,21], but so far no study has identified specific genetic loci that may be involved.

Two models were suggested for the mechanism that creates a colony specific CHC profile[22]. In the colony Gestalt odour model, cuticular lipids are being transferred and mixed between colony members during allogrooming and/or trophallaxis (transfer of food)[6,23,24]. This serves to reduce intra-colony variability, allowing for nestmate recognition. The alternative model is the individualistic model, in which all CHCs found on an individual are self-produced and there is no significant transfer among colony members. Under this model, the similarities between nestmate CHCs profiles may be explained by shared genetics between the closely related colony members and by their shared environment. These two alternative hypotheses were examined in multiple studies, and evidence for both models was collected. For example, colonies of *Cataglyphis Iberia* ants were divided to two groups, and this resulted in the divergence of the groups' CHC profiles and the increased inter-group aggression[25]. The CHCs profiles converged after the separated groups were reunited, as expected under the Gestalt model of shared CHC relative quantities. In another study of *Rhytidoponera confuse* ants, levels of aggression towards nestmates were measured after members of two colonies were caged together[26]. The study concluded that the individualistic component is a greater contributor to the colony chemical identity than the homogenizing Gestalt effect.

The uniform CHCs profile of a colony is a colony-level phenotype, a phenotype which is the combined output (the average or any other function) of the individual phenotypes of nestmates. As with any other phenotype, colony-level phenotypes may be affected by internal factors such as genetics, epigenetics, animal size, and its health, and external factors such as nest material, diet, predation pressure, weather, and seasonality. Other examples of colony-level phenotypes in social insects include alternative social structures, such as the monogyne or polygyne social structures in fire ants[27], collective activities such as foraging and nest construction[28–30] , and social immunity, the defensive actions taken against pathogens and parasites[29,31,32]. In ants and other eusocial insects, a colony is typically made of close relatives that may be regarded as a single colonial organism or a superorganism[33,34]. Therefore, it is useful to consider a colony-level genotype as a high-polypy genotype of a superorganism. These collective genotypes may be studied for their association with any collective colony phenotype, in our case, the homogenized CHCs profiles.

Here, we carried out the first Genome Wide Association Study (GWAS) in the search for genetic basis for among-colony variation in CHCs in colonies of *Cataglyphis niger* ants. Based on a pilot study on the power of alternative approaches for executing a colony-level GWAS[35], we sampled 47 colonies of *C. niger* and fully sequenced the genomes of six workers from each colony. We tested for association between genomic polymorphism and the quantities of 34 CHCs in two types of analyses. The first was a regular GWAS study of individual genotypes and phenotypes. We then conducted a colony-level GWAS, motivated by the Gestalt model. In the second analysis, we looked for associations between the colony-level genotypes, represented by the colonial allele

frequency in each locus, and colony-level (averaged) CHCs profiles. These analyses revealed loci that underlie inter-colony variation in CHCs profiles, which constitute the genomic basis for nestmate recognition cues in ants.

Methods

6.3.1 Sampling

Ants were collected between April 24 and May 10, 2016 from nests dug along a 4 km transect in Betzet beach on the northern Israeli coastline (from to N33.07868, E35.10705 to N33.05162, E35.10245; see Sup. Figure S1). This population was previously referred to as *Cataglyphis drusus*[36], but our recent species delimitation study suggested that this is the same species as *C. niger*, because these populations are not differentiated by their nuclear genomic DNA[37]. Colonies of this population are monogyne (headed by a single queen) and polyandrous (queens are multiply mated)[36,38]. A monogyne, polyandrous population in this species has a mean within-colony genetic relatedness of 0.26. We collected at least 30 ants from each of 50 nests, 47 of which were used in this study (N35.10297, E33.05339 - N33.05162, E35.10245). The other three nests were used in the pilot stage of this GWAS[35].

6.3.2 Whole genome sequencing

For six individuals from each of the 47 nests, DNA was extracted from the head and abdomen (QIAGEN AllPrep DNA/RNA Mini kit) and the thorax was used for the chemical analysis of CHCs (see below). A uniquely barcoded genomic library was constructed for each sample following the standard protocol of the Illumina TruSeq Nano DNA Library Prep kit. Briefly, a Covaris S220 sonicator was used for DNA shearing aiming for 550bp inserts, ends were repaired, and the fragments were size-selected and purified using

magnetic beads (supplied in kit). Then, an adenosine was added to the 3' end of the blunt fragments, individually barcoded adaptors were ligated, and ligated fragments were amplified (eight PCR cycles). Libraries were pooled at equal quantities as three separate pools, each of which was sequenced in two lanes of a paired-end, 150bp reads, on a HiSeq X Ten Illumina sequencer (six lanes in total).

6.3.3 Sequence data processing and genotype calling

Raw reads pre-processing

Whole-genome sequence data were successfully obtained for 276 of the 282 worker samples (four from colony 10, five from colonies 18, 19, 22 and 29 and six from each of the other colonies). A total of 5,941,275,998 reads of 150bp were sequenced, with an average of 21,526,362 reads per sample, which is an average genome coverage of 12X (0.5X – 28X). Duplicate read pairs were removed and low quality reads and adaptor contaminations were trimmed or removed using Trimmomatic[39] version 0.36, leaving sequences that were at least 75bp long. The total number of remaining reads was 5,527,107,050 (93% of the raw data). Reads were aligned to the *C. niger* reference genome (version Cnig_gn2) using Bowtie2[40] version 2.2.5 run with the default parameters 'very-sensitive' and 'end-to-end'. 3,216,552,155 reads (54% of raw reads) remained after the filtering out alignments with three or more mismatches or multiple mapping, which were defined as reads with a second best match that has less than twice the number of mismatches as the best match. HaplotypeCaller of the Genome Analysis Toolkit (GATK) package[41] version 3.7 was used to create a Single Nucleotide Polymorphism (SNP) catalogue containing 2,792,460 SNPs.

In a first stage of filtering, we removed indels and SNPs with more than two alleles from the catalogue, leaving 2,413,918 SNPs. 16 samples (all four of colony 10, three of colony 11, two of colony 9 and one of colonies 2, 8, 15, 16, 25, 40 and 42) were removed because they were missing genotype data in more than 50% of the loci, leaving 260 individuals from 46 colonies in the analysis.

SNPs catalogue for GWAS

In a second stage filtering we required for each locus to have genotype calls for at least 80% of the samples with a minimum number of 6 reads per genotype call, a maximum of 250, and a minimum minor allele frequency (MAF) of 15%. In order to remove false SNPs that are the result of collapsed repetitive sequences in the reference genome assembly, a control for these was made using three haploid male *C. niger* sampled in Betzet Beach (33°4'40.88"N/35°6'33.97"E) that were fully-sequenced with high coverage (177X, 55X and 72X). This was done by creating a blacklist of loci where one or more of these haploid samples appears to be heterozygous, which indicates an artifact because male ants are haploid. All SNPs within 600 bp of such heterozygous loci were removed from the catalogue. Additionally, excessively covered SNPs, defined as loci with an average number of reads per sample > 20 (average genome coverage + 2 x standard deviation – see supplementary Figure S2a). We then removed 14 samples that had more than 60% missing genotypes after this filtering, and as a result had to exclude colony 9 because it had only two samples left. We were left with 244 individuals from 45 colonies (three from colony 11 and 29, four from colony 7, 8, 25 and 32, five from colonies 2, 14, 15, 16, 18, 19, 20, 22, 26, 30, 40 and 42 and six from all the rest) and 171,570 SNPs. The average coverage of this filtered SNP catalogue across the

remaining 244 individuals was 10.2X (calculated by the actual number of reads covering the SNPs). Overall, 6,348,274 (15.2%) of all possible 41,863,080 locus X sample combinations did not have genotype call (missing data).

Colonial genotype processing and calculation

For the colony-level analysis, we required that every locus had genotype calls in at least three individuals in each colony, further reducing the number of SNPs to 171,355. Overall, 659,721 (8.6%) of possible 7,710,975 locus X colony combinations did not have genotype call (missing data). We defined colony-level genotypes as the estimated allele frequency of the colony at every locus, which essentially means that a colony is treated as a single polyploid organism. For example, if the genotypes of six members of a colony are 00, 01, 01, 11, 11, 11, where 0 and 1 represent the two alternative alleles in a locus, their individual genotypes were coded in the input file for the GWAS analysis as 0, 1, 1, 2, 2, 2 and their colony-level genotype was calculated as an average: $\frac{(0+1+1+2+2+2)}{6} = 1\frac{1}{3}$.

6.3.4 Kinship inference

Individual-level kinship based on the whole-genome data

To create the kinship matrix on the individual-level, we continued to filter the SNP catalogue of the whole-genome sequenced samples (after first stage filtering) so each locus had genotype calls in at least 88% of the samples with a minimum of 6 reads, a maximum of 250, and a minimum MAF of 1% (a minimum of two individuals that share the minority allele). We controlled for and filtered out reads that were mapped to suspected collapsed repetitive sequences in the reference as described above, and

similarly removed 16 samples from the analysis due to insufficient genotype calls. This resulted in a catalogue of 88,238 SNPs. Using the program Beagle[42], we imputed and phased the catalogue to the total of 9,634 phased segments. The identity-by-descent (IDB) method implemented in refined-IBD[43] was used to identify shared IBD haplotypes between the samples. A kinship matrix was created based on the total length of IBD haplotypes shared between every pair of samples.

Colony-level kinship based on RAD-sequencing

To better estimate kinship between colonies, one individual from each of the 47 colonies was chosen to be RAD sequenced with high coverage.

Restriction-site associated DNA (RAD) sequencing

For one worker per nest, a reduced representation genomic library was constructed according to a modified double-digest Restriction-site Associated DNA sequencing (ddRAD-seq) protocol, based on protocols from Parchman *et al.*[44] and Buerkle *et al.*[30]. Briefly, DNA was digested by two different restriction enzymes (EcoRI as the rare-cutter; MseI as the frequent-cutter) and ligated to barcoded adaptors for multiplexing. Products were amplified using Q5 Hot Start Polymerase (NEB), with the number of cycles reduced to 20, the number of replicates increased to four, and starting DNA volume increased to 6ul. Also, primers and dNTPs were added to the final thermal cycle in order to minimize single-stranded or heteroduplex PCR products. The libraries were sequenced in one lane of a paired-end, 150bp reads, on a HiSeq X Ten Illumina sequencer.

Pre-processing of RAD-seq data

A total of 823,087,220 reads were sequenced from 47 workers (one from each of the colonies), which is an average expected depth of 65X (14X – 105X) based on the number of restriction sites in the reference genome. The raw reads were initially processed using the *Stacks* pipeline version 2.2[45]. Low quality reads were discarded if their quality score dropped below an averaged phred score of 10 in a sliding window of 15% of the reads' length. After this initial processing, 736,899,655 reads that were assigned to a sample remain (90% of raw data). The reads were mapped to the reference genome of *C. niger* (version Cnig_gn2) using *Bowtie2* and filtered using the same criteria as for the whole-genome data above. After this filtering, 718,157,408 alignments remained. We continued to analyse the mapped sequences using the *gstacks* program of the *Stacks* pipeline and created a catalogue containing 90,006 SNPs for the 47 samples.

Combining the catalogue additional samples from across Israel

To increase the number of samples and thereby improve SNP calling, imputation and phasing, we made use of another data set that included 103 RAD-sequenced *C. niger* and *C. israelensis* individuals sampled across Israel (described in Rainer-Brodetzki et al. (2019)[37]). The combined catalogue that was created from the 150 individuals contained 346,940 SNPs.

The following filtering parameters were used: each locus was required to have a genotype call in at least 90% of the samples, with the minimal number of reads of 3, a maximum of 4000, and had a minimum MAF of 1.5%. We controlled for collapsed repetitive elements by using the black list described above and by removing excessively

covered SNPs, which were defined as loci with a mean number of reads > 250 (mean coverage + 2 x standard deviation – see supplementary Figure S2b). After filtering, 21,179 polymorphic sites remained in the combined catalogue.

Colony-level kinship inference based on RAD-seq data

As with the whole-genome data, the RAD-seq SNP catalogue was imputed and phased using Beagle[42] and refined-IBD[43] to a total of 502 phased segments across the genome. Shared IBD haplotypes between individuals were identified and a kinship matrix was created based on the total length of IBD haplotypes shared between every pair of samples representing 47 colonies.

6.3.5 STRUCTURE between colonies

We used STRUCTURE[46,47] to investigate population structure in our samples. As prepartion for the population structure analysis, we filtered the RAD based SNPs catalog further. For each locus, we required genotype calls in at least 95% of the samples in each population (i.e. less than 5% missing data); a minimum of three reads made for a genotype call. Additionally, we required a MAF of 0.5%. This stringent filtering resulted in a collection of 13,526 high confidence SNPs.

We ran STRUCTURE over K (number of expected clusters) values of 2–10, 100 times for each K, with 100 different sets of 1000 SNPs randomly chosen out of the high confidence SNPs collection, a total of 900 separate runs. To avoid linked sites from affecting the analysis, we required a distance of at least 3000 bp between the selected sites. Multiple runs over various data subsets contributed to the robustness of the clustering inference and allowed us to use more SNPs than would be possible in a single

run. We ran STRUCTURE for 500,000 MCMC repetitions and discarded the first 20,000 (burn-in period). All the other parameters were kept at default values. The results were analyzed and united to a concensus population structure depending on K using CLUMPAK[48].

6.3.6 Chemical analysis of cuticular hydrocarbons

Cuticular hydrocarbon (CHC) analysis

CHCs were measured for the same six workers from each of the 47 nests that were used for genomic sequencing. Thoraces were individually immersed in hexane to extract non-polar cuticular lipids from each sample separately. Initial analysis was conducted by gas chromatography/mass spectrometry (GC/MS), using a VF-5ms capillary column, temperature-programmed from 60◦C to 300◦C (with 1 min initial hold) at a rate of 10◦C per min, with a final hold of 15 min. Compounds were identified according to their fragmentation pattern and respective retention time compared to authentic standards. Subsequently, all samples were assayed quantitatively by flame ionization gas chromatography (GC/FID), using the above running conditions. Peak integration was performed using the program Varian Galaxie 1.9. and relative amounts of each compound were calculated. The relative amounts of each CHC were calculated for each sample. For the colony-level analysis, the relative amounts were averaged between the members of each colony.

Normalization of the CHC relative amounts

Outliers to the distribution of each CHC in each of the two datasets (individual relative amounts and averaged colony relative amounts) were removed. These were defined as the amounts that were 1.5 times higher or 1.5 times lower than the interquartile range

(the difference between the 75th and 25th percentiles of the distribution). For each dataset, we normalized the distribution of the remaining values using the R package *bestNormalize*[49], which chooses the most fitting normalization function for the dataset on the basis of the Pearson P test statistic for normality. See Supplementary Table1 for more details.

6.3.7 Genome Wide Association Study of nestmate recognition

In order to test for a genetic basis of variation in CHC, we conducted a Genome Wide Association Study (GWAS) over the relative amounts of each CHC, in two levels. The first is the individual-level, in which we used the catalogue of genotypes created for the 244 samples in 45 colonies, as described above, and their relative amounts of CHC. The second level is the colony-level, in which we used the catalogue of colony-level genotypes created for the 45 colonies, as described above, and their averaged colony-level CHC relative amounts.

The standard practice for GWAS is the use of a Mixed Linear Model (MLM), in which the population structure and the genetic variation are represented as fixed effects, and kinship between samples as random effects. Here, for each dataset (individual- or colony-level), we to accounted for samples relatedness by the respective kinship matrix (whole-genome or RAD sequencing data for the individual- or colony-level datasets, respectively) and for population structure by a Principle Component Analysis (PCA) of the SNPs over 45 dimensions in the individual-level analysis and 8 dimensions in the colony-level analysis. The number of dimensions was chosen based on the fit of quantile-quantile (Q-Q) plots – see below.

Execution of GAPIT

Genomic Association and Prediction Integrated Tool (GAPIT)[50] is an R package which executes the Efficient Mixed Model Association (EMMA)[51] method, a computationally efficient algorithm for the study of genomic association using MLM. We ran the program for each CHC in each dataset separately using the Multiple Loci Mixed Linear Model (MLMM), which is implemented in GAPIT by a forward-backward stepwise MLM regression. In each step, the loci that were found to be significantly associated with the trait in the former step are added to the model as cofactors. Accounting for the effect of multiple loci on the trait reduces residual variation in the trait and allows for a greater statistical power in QTL detection. We evaluated how well the model accounts for population structure and kinship using Q-Q plots: plotting the negative logarithm of the assessed *p*-values and comparing them to the expected distribution of *p*-values under the null hypothesis of no association, as calculated by GAPIT. See supplementary Figure S3. Of the 171,570 / 171,355 loci analysed, 155,815 / 155,807 were mapped to a linkage group on the genetic map[52].

Empirical permutation test

To account for additional unknown confounding factors and other potential problems in the model that might lead to false inference of association, we performed a permutation test to empirically calculate a null distribution of *p*-values when no association between the genotype and phenotype exists: for each CHC, we randomly shuffled the trait values between the samples. Using the shuffled traits and leaving the other model parameters unchanged, we rerun GAPIT 100 times. We did this for both the individual-level and colony-level analyses. For each trait, the original *p*-values of the original run were re-

evaluated by comparing them to the distribution of the *p*-values in the shuffled datasets. The *p*-values were further corrected for multiple testing using the Benjamini Hochberg method[53].

Results

We conducted a GWAS to identify the genetic basis of variation in CHCs. We used the MLMM model implemented in GAPIT to test association between the relative amounts of 34 CHCs and genotype calls at 171,570 SNPs identified through the whole-genome sequencing of 244 workers from 45 colonies of *C. niger* (3 – 6 ants from each colony). As part of the analysis, relatedness between samples is accounted for by a kinship matrix, inferred by identity-by-decent (IBD), and population structure is accounted for using PCA. This analysis was run both at the individual-level and at the colony-level, where the colony phenotype was defined as the averaged CHC level in the colony and the colony genotype as the allele frequency in the colony. Each locus was assigned with a *p*-value for its association with each of the traits under the model implemented in GAPIT. These *p*-values were compared to the distribution of *p*-values under the null model of no association between genotypes and phenotypes, which was empirically calculated by shuffling trait values between the samples. This shuffling procedure produced so-called "empirical *p*-values", which we further corrected for multiple testing using the FDR method.

6.4.1 Colonies population structure and kinship between samples

Colonies population STRUCTURE

We inferred population structure from RAD-seq of one sample from each of the 47 colonies using the program STRUCTURE. This analysis revealed spatial clustering of the northern and southern colonies (Figure 6.1). This indicates limited dispersal during mating flights. STRUCTURE results for K=2 and K=3 are presented in Figure 6.1. Higher K values results in the assigning of individuals to several different clusters and do not appear indicative of true population structure.

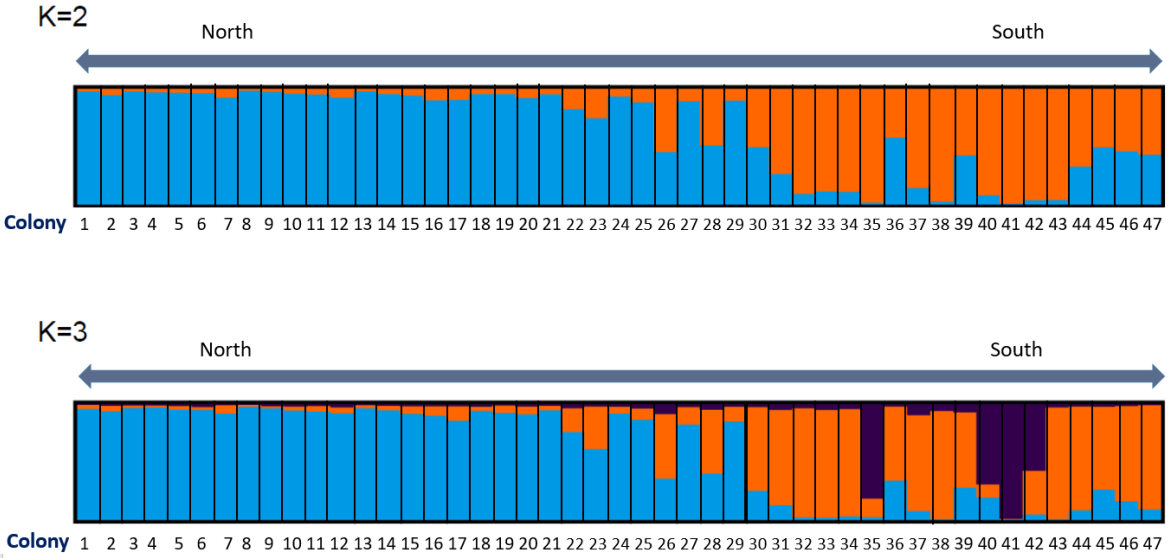

Figure 6.1. **STRUCTURE results for K=2 and K=3**. A north-south (blue-orange) spatial differentiation is evident from the assigned clustering. The lower a colony number is, the northern it is located.

Individual-level kinship

Kinship among samples was inferred from the whole-genome sequencing data based on the total length of shared IBD haplotypes (Figure 6.2a). As expected, and with very few exceptions, stronger kinship was identified between sample collected from the same nest (intra-colony kinship) relative to kinship between nests (inter-colony kinship). Intra-colony kinship was not detectable in colonies 26, 28, 29 and 37. Some of the samples in

these colonies have high proportions of missing data, which may result in low kinship detection power. The inter-colony kinship between members of colonies 33 and 47 was found to be similar to intra-colony kinship, indicating that the queens of these two colonies were probably closely related, either a mother and a daughter (50% related) or full sisters (75% related). This is also true for some members of colonies 40, 41 and 42. There also appears to be some kinship among colonies 1 – 20 (northern part of the transect) and among colonies 32 – 47, in line with the clustering of colonies that was observed in the STRUCTURE results.

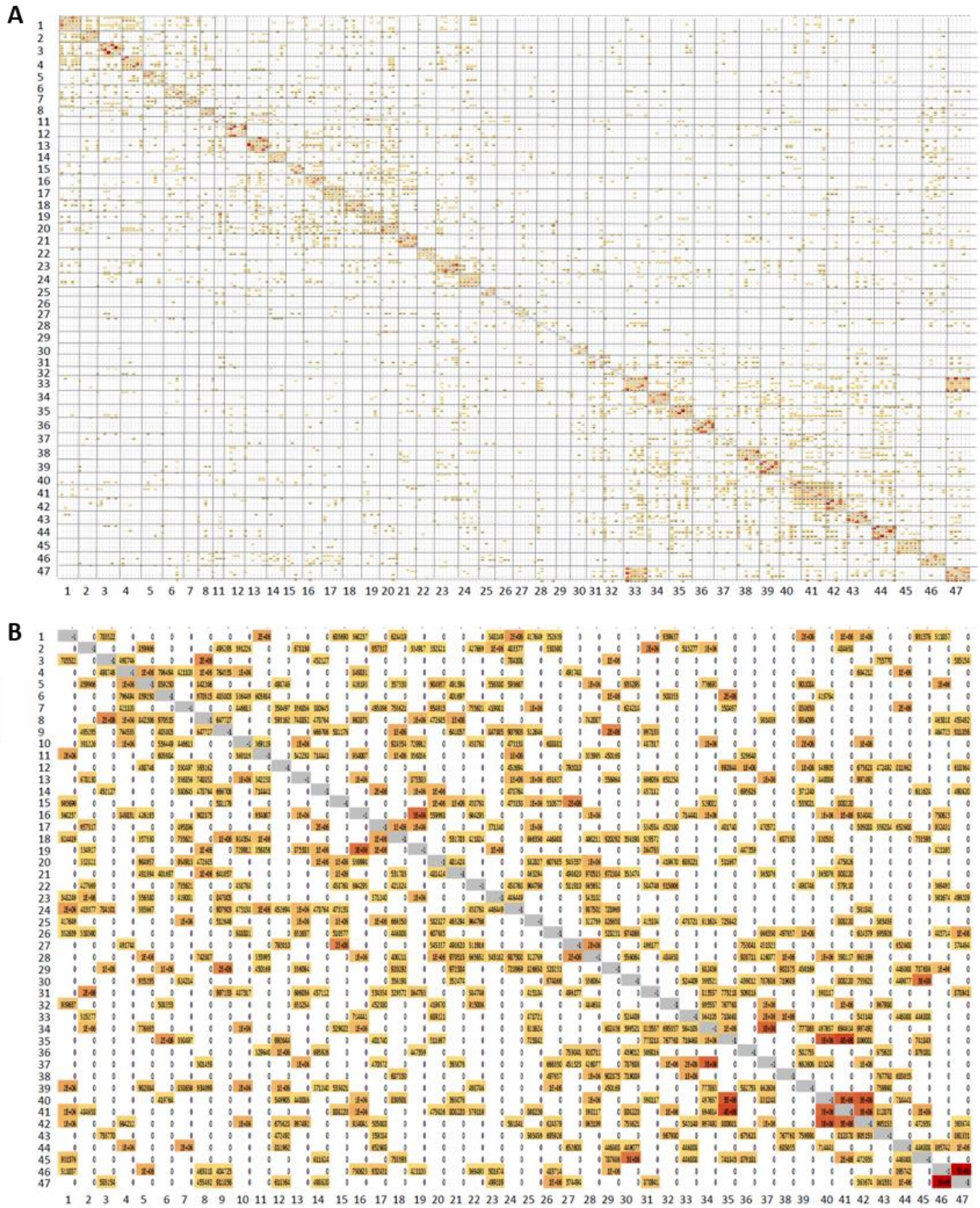

Figure 6.2. Kinship matrices based on lengths of shared haplotypes between 244 individuals of 45 colonies (A) and 47 individuals of 47 colonies (B). For visability, only colony numbers are presented. The values are the total numer of bases on shared happlotypes between each pair of samples. Higher values are stronger red.

6.4.2 Colony-level kinship

Kinship among colonies was also inferred from the more deeply sequenced RAD-seq data from one representative of each colony. This analysis did not show the north-south clustering pattern. Various levels of inter-colony kinship were observed, mostly between neighbouring nests, which also supports the hypothesis of short range dispersal. High kinship values were detected between colonies 16 and 19, colonies 34 and 37, colonies 35, 40, 41 and 42 (though not between colonies 35 and 42), and colonies 46 and 47 (Figure 6.2b). We note that the strong kinship signal among colonies 40, 41 and 42 is consistent between the colony-level kinship inferred from the RAD-seq data and the individual-level kinship inferred from the whole-genome data.

6.4.3 Individual-level GWAS

The individual-level GWAS identified 13 QTLs that were found to be associated with one of the CHC with the corrected q-value < 0.1 (FDR corrected p-values), three of which were mapped to genes (Figure 6.3 and Table 6.1). Two of the QTLs found associated with 5Me-C25 were only 4.6cM apart of on chromosome 15. Additionally, 69 loci were found to be associated with one of the traits with a q-value < 0.3. Of these, 22 were located within a gene or within 2000 bp upstream from a gene's start codon (gene hits).

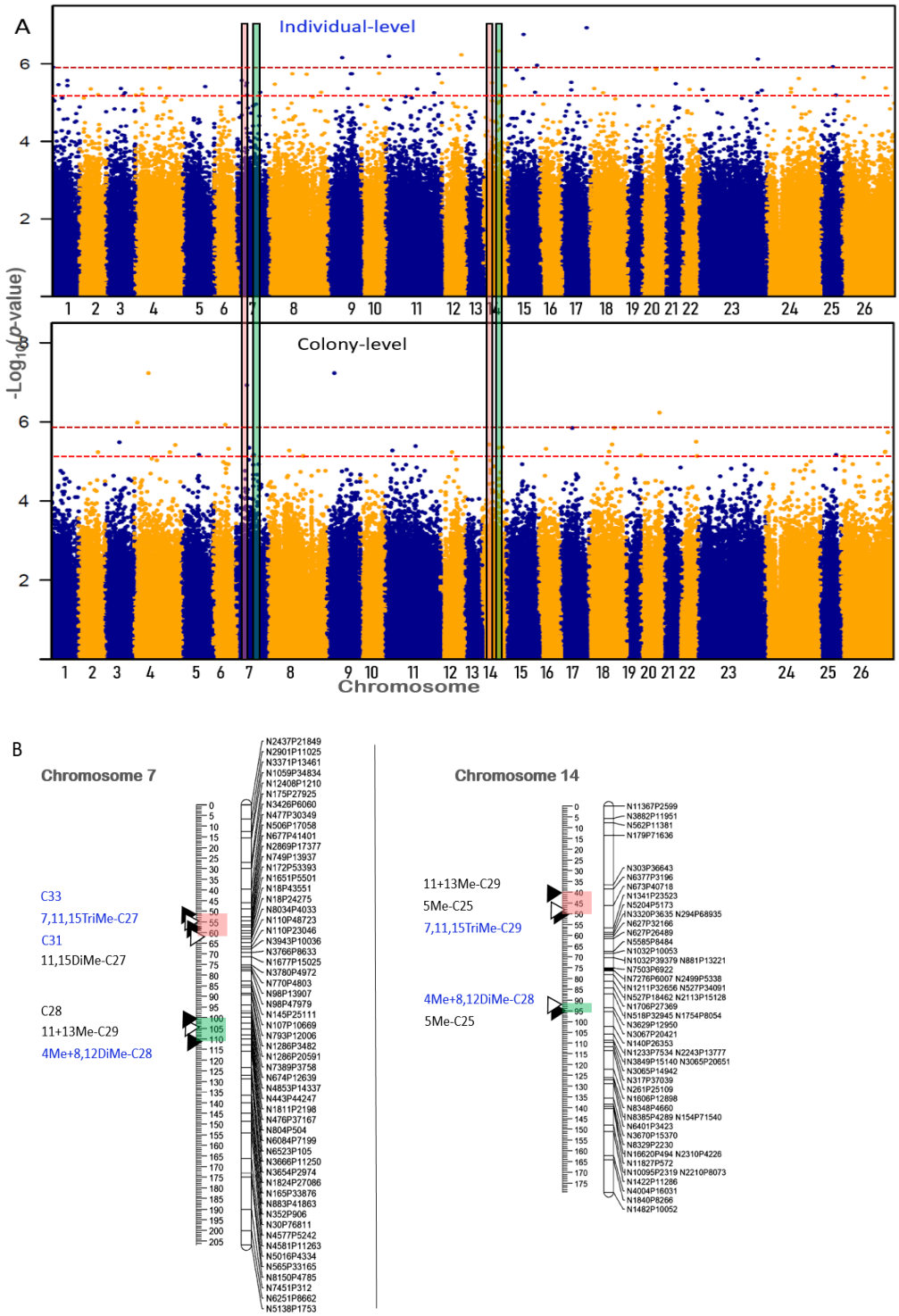

Figure 6.3. Manhattan plots of loci *p*-values associated with the CHCs GWAS. Individual-level is A above and colony-level is A below. Loci above the maroon dotted line are statistically significant with FDR of 10%. Loci above the red dotted line are statistically significant with FDR of 30%. Four QTL clusters with QTLs identified in the individual-level and in the colony-level analyses are marked on chromosomes 7 and 14 and presented in detail (B). The associated CHCs are shown in the order of their appearance on the chromosome (individual-level QTLs in blue and colony-level QTLs in black)

Table 6.1. Loci and genes that were found to be associated with CHCs in the individual-level GWAS

CHC	*q*-value threshold				Genes (*q*-value)
	< 0.05	< 0.1	< 0.2	< 0.3	
3Me-C25	-	-	-	4	Discoidin domain-containing receptor 2 (0.282)
5Me-C25	2	4	7	7	Sodium-coupled monocarboxylate transporter 1 (0.106)
					Protein Wnt-10a (0.106)
					2-oxoglutarate and iron-dependent oxygenase domain-containing protein 3 (0.093)
					MIP18 family protein galla-1 (0.093)
4,12DiMe-C26	-	-	2	5	Putative sperm flagellar membrane protein (0.280)
11+13Me-C27	-	-	1	1	Putative protein (0.173)
7,11,15TriMe-C27	1	1	4	8	DDB1- and CUL4-associated factor 5 (0.018)
					Troponin I (0.265)
12Me-C28	-	3	3	5	Follistatin (0.094)
4Me+8,12DiMe-C28	-	1	4	10	Pyridoxal-dependent decarboxylase domain-containing protein 1 (0.211)
					39S ribosomal protein L12, mitochondrial (0.211)
					Putative protein (0.211)
					Putative protein (0.168)
C29	-	-	2	5	Protein phosphatase Slingshot homolog 1 (0.285)
7,11,15TriMe-C29	-	-	-	3	Putative protein (0.254)
2Me-C30	-	-	1	4	
4Me-C30	-	1	1	1	
C31	-	-	8	9	Cadherin-99C (0.144)
					Kinesin-like protein KIF6 (0.144)
					Putative protein (0.144)
					Putative protein (0.226)
C32	-	3	5	5	Putative protein (0.091)
C33	-	-	-	2	Domain of unknown function (0.282)
All	3	13	39	69	

6.4.4 Colony-level GWAS

The colony-level GWAS identified three QTLs that were found to be associated with 5Me-C25, two of which with *q*-value < 0.05 (Figure 6.3 and Table 6.2). These QTLs were located on different chromosomes than the significant loci identified in the individuals-

level analysis. Two additional QTLs were found to be associated with two other CHCs. There are 30 QTLs that with a *q*-value < 0.3 that were found to be associated with CHCs, of these, six were gene hits.

Table 6.2. Loci and genes that were found to be associated with CHCs in the colony-level GWAS.

CHC	*q*-value threshold				Genes (*q*-value)
	< 0.05	< 0.1	< 0.2	<0.3	
5Me-C25	2	3	6	7	Sterile alpha and TIR motif-containing protein 1 (0.142)
11+13Me-C27	1	1	1	3	Aminopeptidase N (0.276)
11,15DiMe-C27	1	1	1	4	Protein TANC2 (0.298)
C28	-	-	-	7	Progestin and adipoQ receptor family member 4 (0.227)
					Protein gooseberry-neuro (0.261)
11+13Me-C29	-	-	7	8	Claudin_2^PMP-22/EMP/MP20/Claudin tight junction (0.233)
3Me-C29	-	-	1	1	
All	4	5	16	30	

Put together, 99 QTLs were found to be associated with CHCs with *q*-value < 0.3. The QTLs distribution across the genome was found to be significantly different than a uniform distribution in a Kolmogorov-Smirnov test (D = 5038.9, *p*-value < 2.2×10^{-16}). We identified 13 clusters of two to four loci that were within 10cM long from each other. Seven of the clusters included QTLs from both individual- and colony-level analyses (Supplementary Table S3). Overall, 32 of the 99 QTLs were in clusters. There were additional three clusters, each containing 2 QTLs that were more than 10cM but less than 12cM from each other.

Of the gene hits, many are involved in metabolism of amino acids. For example, pyridoxal-dependent decarboxylase domain-containing protein 1 contains a QTL for

4Me+8,12DiMe-C28. Other QTL genes are regulatory factors such as protein phosphatase Slingshot homolog 1 for C29.

Discussion

We executed GWAS for ant CHCs profile using two approaches to GWAS, individual level and colony level. We detected one or more putative QTLs for 18 of the 34 CHCs (*q*-value < 0.3): 14 in the individual-level analysis and six in the colony-level analysis. Two CHCs appeared in the results of both analyses (5Me-C25 and 11+13Me-C27). For the remaining 16 CHCs, either their QTLs were missed due to problems in the analysis itself, such as measuring or sequencing errors, wrong model choice, inaccurate kinship matrices, etc., or because the contribution of genetics to their quantitative variations was too low to be detected with limited statistical power of GWAS using a sample size of 45 colonies. Nevertheless, this is the first report of QTLs for CHC in any ant species.

While neither the individual- nor the colony-level analysis identified the same locus as being associated with a CHC more than once, oftentimes QTLs of different CHCs were found close by or in the same genetic position in the linkage map. It has been shown that different coding regions across the chromosome may form separate compartments in regards to functionality, which imply their co-regulation[54,55]. We hypothesize that the genomic clusters we identified may be topological or functional domains that are related to the synthesizing of CHCs. Insects synthesize hydrocarbons by elongating fatty acyl-CoA precursors to produce long chain fatty acids that are then converted to hydrocarbons by the removal of the carboxyl group[8]. The elongation reaction is responsible for regulating hydrocarbons lengths[56] and thereby in determining the

variation in quantities of various CHC with a range of chain lengths. Shared QTLs between CHCs may be related to such a mechanism. Further study of the identified QTLs is needed in order to examine their relation to CHC synthesis and elongation.

The ability to discriminate between nestmates and non-nestmates depends on the differences between their CHCs profiles. The more distinct their colony CHCs profile is, the easier it is for nestmates to identify each other. Colonies with rare genotypes would therefore be favoured by natural selection over colonies with common genotypes. Rare alleles would be selected for so long they are rare, thus maintaining and increasing the polymorphism in the population. We suggest that balancing (frequency-dependent) selection is acting on genes that regulate CHCs, in similar fashion to other recognition systems for which polymorphism is advantageous for the discrimination of self vs. non-self, such as the MCH immunity system in mammals[57,58] and the Self-Incompatibility system in plants[59]. This leads us to predict that the variation in CHCs relative amounts will increase in evolution through the generation of polymorphic genetic loci that affect CHC synthesis and/or their secretion on the cuticle, i.e. QTLs.

Despite this prediction for the importance of genetic polymorphism in the evolution of nestmate recognition, environmental factors may have greater contribution than genetics factors to the phenotypic variation. In our analysis, only seven QTLs for four of the 34 CHCs were detected with a q-value < 0.05; two CHCs in the individual- and three in the colony-level analysis (QTLs for CHC 5Me-C25 were detected in both analyses). Diet was shown to influence the cuticular chemical profiles in the polygyne (multiple queens) and polydemous (multiply mated) colonies of *Formica aquilonia* ants, where

nestmates are not necessarily related[18]. In comparison, the colonies of *C. niger* used in this study are monogyne and polydemous[38], and so our samples were closely related (at least 25% related). Environmental odours also appear to determine aggression levels between lab-reared and field-collected workers of monogyne *Solenopsis invicta* colonies[19] and similarly between lab-reared and field-collected polygyne *Rhytidoponera confusa* workers[17].

Next to genetics and the environment, the Gestalt model suggests that social interaction between colony members has an important role in determining colony identity. Social interactions have substantial impacts on many other phenotypes in insect societies. For example, when *Camponotus floridanus* workers were fed with juvenile hormone, an important regulator of growth and development in insects, the larvae they fed through trophallaxis were twice as likely to become larger workers[60]. In termites, social interactions of allogrooming and trophallaxis appear to contribute in determining the caste of developing brood[61]. The physical transfer and mixing of CHCs between nestmates may be a major factor shaping their CHCs identity. In our colony-level analysis, CHCs transfer between nestmates is accounted for by the averaging out of nestmate genetics and their CHCs phenotypes. This analysis resulted in less QTLs identified in comparison to the individual-level analysis, but in general with greater statistical significance, indicating more confidence in the colony-level model. This result is in line with the Gestalt model. Alternatively, it may be that the averaging of colonies' genotypes and phenotypes helps in eliminating noise introduced in the chemical analysis and sequencing/genotype errors, and so results in a more robust outcome. Additional

behavioural and experimental studies are needed to provide further support to the Gestalt model and determine the exact nature of social effects on CHC profiles.

References

1. Hamilton, W. D. The genetical evolution of social behavior. I. *Gr. Sel.* 23–43 (1964).
2. Hamilton, W. D. The evolution of social behavior II. *Journal of Theoretical Biology* **7**, 17–52 (1964).
3. Errard, C. & Hefetz, A. Label familiarity and discriminatory ability of ants reared in mixed groups. *Insectes Soc.* **44**, 189–198 (1997).
4. Dani, F. R. *et al.* Nestmate recognition cues in the honey Bee: Differential importance of cuticular alkanes and alkenes. *Chem. Senses* **30**, 477–489 (2005).
5. Lahav, S., Soroker, V., Hefetz, A. & Vander Meer, R. K. Direct behavioral evidence for hydrocarbons as ant recognition discriminators. *Naturwissenschaften* **86**, 246–249 (1999).
6. van Zweden, J. S. & d'Ettorre, P. Nestmate recognition in social insects and the role of hydrocarbons. *Insect Hydrocarb. Biol. Biochem. Chem. Ecol.* 222–243 (2010). doi:10.1017/CBO9780511711909.012
7. Vernier, C. L. *et al.* The cuticular hydrocarbon profiles of honey bee workers develop via a socially-modulated innate process. *Elife* **8**, 1–27 (2019).
8. Blomquist, G.J., Bagnères, A.-G. Insect Hydrocarbons: Biology, Biochemistry and Chemical Ecology. *Cambridge Univ.* (2010).
9. Martin, S. & Drijfhout, F. A review of ant cuticular hydrocarbons. *J. Chem. Ecol.* **35**, 1151–1161 (2009).
10. Howard, R. W. chemical ecologyand biochemistry of insect HYDROCARBONS. *Annu. Rev. Entomol.* (1982).
11. Howard, R. W. & Blomquist, G. J. Ecological, behavioral, and biochemical aspects of insect hydrocarbons. *Annu. Rev. Entomol.* **50**, 371–393 (2005).
12. Blomquist, G. J., Tittiger, C. & Jurenka, R. *Cuticular Hydrocarbons and Pheromones of Arthropods*. *Hydrocarbons, Oils and Lipids: Diversity, Origin, Chemistry and Fate* (2018). doi:10.1007/978-3-319-54529-5_11-1
13. Wagner, D., Tissot, M., Cuevas, W. & Gordon, D. M. Harvester ants utilize cuticular hydrocarbons in nestmate recognition. *J. Chem. Ecol.* **26**, 2245–2257 (2000).
14. Drescher, J., Blüthgen, N., Schmitt, T., Bühler, J. & Feldhaar, H. Societies drifting apart? behavioural, genetic and chemical differentiation between supercolonies in the yellow crazy ant anoplolepis gracilipes. *PLoS One* **5**, 1–8 (2010).
15. Foitzik, S., Sturm, H., Pusch, K., D'Ettorre, P. & Heinze, J. Nestmate recognition and intraspecific chemical and genetic variation in Temnothorax ants. *Anim. Behav.* **73**, 999–1007 (2007).
16. Blight, O. *et al.* Variation in the level of aggression, chemical and genetic distance among three supercolonies of the Argentine ant in Europe. *Mol. Ecol.* **21**, 4106–4121 (2012).
17. Crosland, M. W. J. Kin recognition in the ant Rhytidoponera confusa I. Environmental odour. *Anim. Behav.* **37**, 912–919 (1989).

18. Sorvari, J., Theodora, P., Turillazzi, S., Hakkarainen, H. & Sundström, L. Food resources, chemical signaling, and nest mate recognition in the ant Formica aquilonia. *Behav. Ecol.* **19**, 441–447 (2008).

19. Obin, M. S. Nestmate recognition cues in laboratory and field colonies of Solenopsis invicta buren (Hymenoptera: Formicidae) - Effect of environment and role of cuticular hydrocarbons. *J. Chem. Ecol.* **12**, 1965–1975 (1986).

20. Teseo, S. *et al.* Genetic Distance and Age Affect the Cuticular Chemical Profiles of the Clonal Ant Cerapachys biroi. *J. Chem. Ecol.* **40**, 429–438 (2014).

21. Menzel, P. P. S. & F. & Abstract. Cuticular hydrocarbons in ants (Hymeno ptera: Formicidae) and other insects: how and why they differ among individuals, colonies, and species. *Myrmecological News* **30**, 1026 (2020).

22. Crozier, R. H. & Dix, M. W. Analysis of two genetic models for the innate components of colony odor in social Hymenoptera. *Behav. Ecol. Sociobiol.* **4**, 217–224 (1979).

23. Beye, M., Neumann, P. & Moritz, R. F. A. Nestmate recognition and the genetic gestalt in the mound-building ant Formica polyctena. *Insectes Soc.* **44**, 49–58 (1997).

24. Beye, M., Neumann, P., Chapuisat, M., Pamilo, P. & Moritz, R. F. A. Nestmate recognition and the genetic relatedness of nests in the ant Formica pratensis. *Behav. Ecol. Sociobiol.* **43**, 67–72 (1998).

25. Lenoir, A. D. and A. Nest Separation and the Dynamics of the Gestalt Odor in the Polydomous Ant Cataglyphis iberica (Hymenoptera , Formicidae). *Behav. Ecol.* **42**, 349–355 (1998).

26. Crosland, M. W. J. Kin recognition in the ant Rhytidoponera confusa II. Gestalt odour. *Anim. Behav.* **37**, 920–926 (1989).

27. Ross, K. G. & Keller, L. Genetic control of social organization in an ant. *Proc. Natl. Acad. Sci.* **95**, 14232–14237 (1998).

28. Beckers, R., Deneubourg, J. L. & Goss, S. Modulation of trail laying in the ant Lasius niger (Hymenoptera: Formicidae) and its role in the collective selection of a food source. *J. Insect Behav.* **6**, 751–759 (1993).

29. Sumpter, D. J. T. & Beekman, M. From nonlinearity to optimality: Pheromone trail foraging by ants. *Anim. Behav.* **66**, 273–280 (2003).

30. Parchman TL, Gompert Z, Mudge J, Schilkey FD, Benkman CW, B. Cajm. Genome-wide association genetics of an adaptive trait in lodgepole pine. *Mol. Ecol.* **21**, 2991–3005 (2012).

31. Macevicz, S. & Oster, G. Modeling social insect populations II: Optimal reproductive strategies in annual eusocial insect colonies. *Behav. Ecol. Sociobiol.* **1**, 265–282 (1976).

32. Huang, Y. C. & Wang, J. Did the fire ant supergene evolve selfishly or socially? *BioEssays* **36**, 200–208 (2014).

33. Trivers, R. L. & Hare, H. Haplodiploidy and the evolution of the social insects. *Science (80-.).* **191**, 249–263 (1976).

34. Henri, J. F, R. J. What is an individual organism? A multilevel selection perspective. *Q. Rev. Biol.* **85**, 1 (2010).

35. Inbar, S., Cohen, P., Yahav, T. & Privman, E. Comparative study of population genomic approaches for mapping colony-level traits. *PLoS Comput. Biol.* **16**, (2020).

36. Eyer, P. A., Seltzer, R., Reiner-Brodetzki, T. & Hefetz, A. An integrative approach to untangling species delimitation in the Cataglyphis bicolor desert ant complex in Israel. *Mol. Phylogenet. Evol.* **115**, 128–139 (2017).

37. Brodetzki, T. R. *et al.* The Interplay between Incipient Species and Social Polymorphism in the Desert Ant Cataglyphis. *Sci. Rep.* **9**, (2019).

38. Brodetzki, T. R. *et al.* The Interplay between Incipient Species and Social Polymorphism in the Desert Ant Cataglyphis. *Sci. Rep.* **9**, 9495 (2019).

39. Bolger, A. M., Lohse, M. & Usadel, B. Trimmomatic: A flexible trimmer for Illumina sequence data. *Bioinformatics* **30**, 2114–2120 (2014).

40. Langmead, B., Trapnell, C., Pop, M. & Salzberg, S. L. Ultrafast and memory-efficient alignment of short DNA sequences to the human genome. *Genome Biol.* **10**, R25 (2009).

41. Aaron McKenna, Matthew Hanna, Eric Banks, Andrey Sivachenko, K. C., Andrew Kernytsky, Kiran Garimella, David Altshuler, Stacey Gabriel, M. D. & DePristo, and M. A. The Genome Analysis Toolkit: A MapReduce framework for analyzing next-generation DNA sequencing data. *Genome Res.* **20**, 1297– 1303 (2010).

42. Browning, B. L., Zhou, Y. & Browning, S. R. A One-Penny Imputed Genome from Next-Generation Reference Panels. *Am. J. Hum. Genet.* **103**, 338–348 (2018).

43. Browning, B. L. & Browning, S. R. Improving the accuracy and efficiency of identity-by-descent detection in population data. *Genetics* **194**, 459–471 (2013).

44. Peterson, B. K., Weber, J. N., Kay, E. H., Fisher, H. S. & Hoekstra, H. E. Double digest RADseq: An inexpensive method for de novo SNP discovery and genotyping in model and non-model species. *PLoS One* **7**, (2012).

45. Catchen, J. M. Stacks: an analysis tool set for population genomics. *Mol. Ecol.* **22**, 3124–3140 (2013).

46. Pritchard, J. K., Stephens, M. & Donnelly, P. Inference of population structure using multilocus genotype data. *Genetics* **155**, 945–959 (2000).

47. Falush, D., Stephens, M. & Pritchard, J. K. Inference of population structure using multilocus genotype data: Dominant markers and null alleles. *Mol. Ecol. Notes* **7**, 574–578 (2007).

48. M., K. N. *et al.* Clumpak: A program for identifying clustering modes and packaging population structure inferences across K. *Mol. Ecol. Resour.* **8**, 444–454 (2016).

49. Peterson RA, C. J. Ordered quantile normalization: a semiparametric transformation built for the cross-validation era. *J. Appl. Stat.* 1–16 (2019).

50. Lipka, A. E. *et al.* GAPIT: Genome association and prediction integrated tool. *Bioinformatics* **28**, 2397–2399 (2012).

51. Kang, H. M. *et al.* Variance component model to account for sample structure in genome-wide association studies. *Nat. Genet.* **42**, 348–354 (2010).

52. Inbar, S., Saied, B., Cohen, P., Frenkel, Z., Pellen, Y., Korol, A., Privman, E. Genetic basis

of cuticular hydrocarbons in the desert ant. *Under review*.

53. Benjamini, Y. & Hochberg, Y. Controlling the False Discovery Rate : A Practical and Powerful Approach to Multiple Testing Author (s): Yoav Benjamini and Yosef Hochberg Source : Journal of the Royal Statistical Society . Series B (Methodological), Vol . 57 , No . 1 (1995), Publi. **57**, 289–300 (1995).

54. Goetze, S. *et al.* The Three-Dimensional Structure of Human Interphase Chromosomes Is Related to the Transcriptome Map. *Mol. Cell. Biol.* **27**, 4475–4487 (2007).

55. Matharu, N. K. & Ahanger, S. H. Chromatin insulators and topological domains: Adding new dimensions to 3D genome architecture. *Genes (Basel).* **6**, 790–811 (2015).

56. Blomquist, G. J., Vogt, R. G. *Insect Pheromone Biochemistry and Molecular Biology*. (Elsevier Academic Press, 2003).

57. Hedrick, P. W. Balancing selection and MHC. *Genetica* **104**, 207–214 (1998).

58. Aguilar, A. *et al.* High MHC diversity maintained by balancing selection in an otherwise genetically monomorphic mammal. *Proc. Natl. Acad. Sci. U. S. A.* **101**, 3490–3494 (2004).

59. Glémin, S. *et al.* Balancing selection in the wild: Testing population genetics theory of self-incompatibility in the rare species Brassica insularis. *Genetics* **171**, 279–289 (2005).

60. LeBoeuf, A. C. *et al.* Erratum: Oral transfer of chemical cues, growth proteins and hormones in social insects (eLife (2016) 5 PII: e51082). *Elife* **8**, (2019).

61. Watanabe, D., Gotoh, H., Miura, T. & Maekawa, K. Social interactions affecting caste development through physiological actions in termites. *Front. Physiol.* **5 APR**, 1–12 (2014).

Supplementary

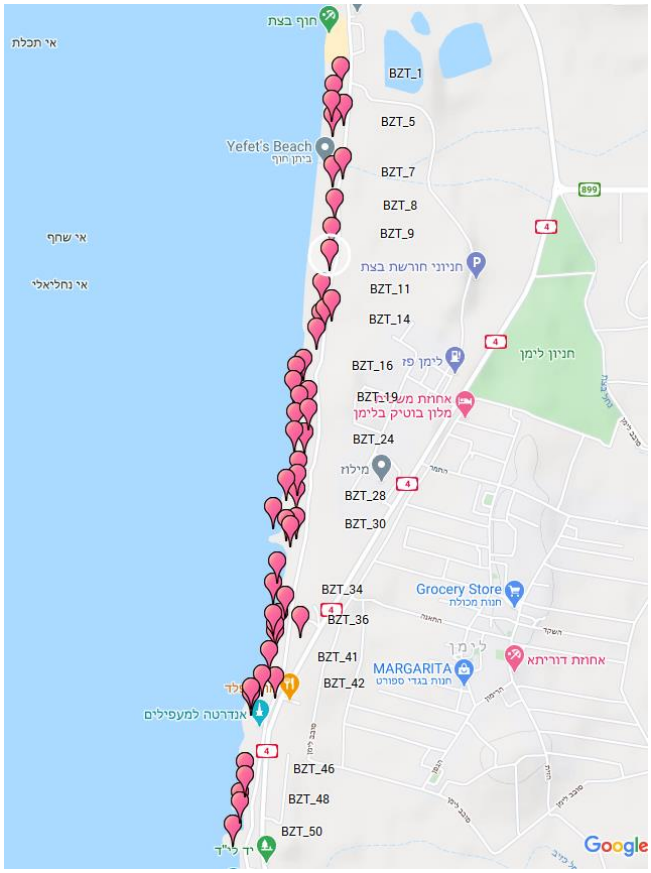

Figure S1. Map of 50 sampled nests along a transact along Betzet Beach in northern Israel (from to N33.07868, E35.10705 to N33.05162, E35.10245).

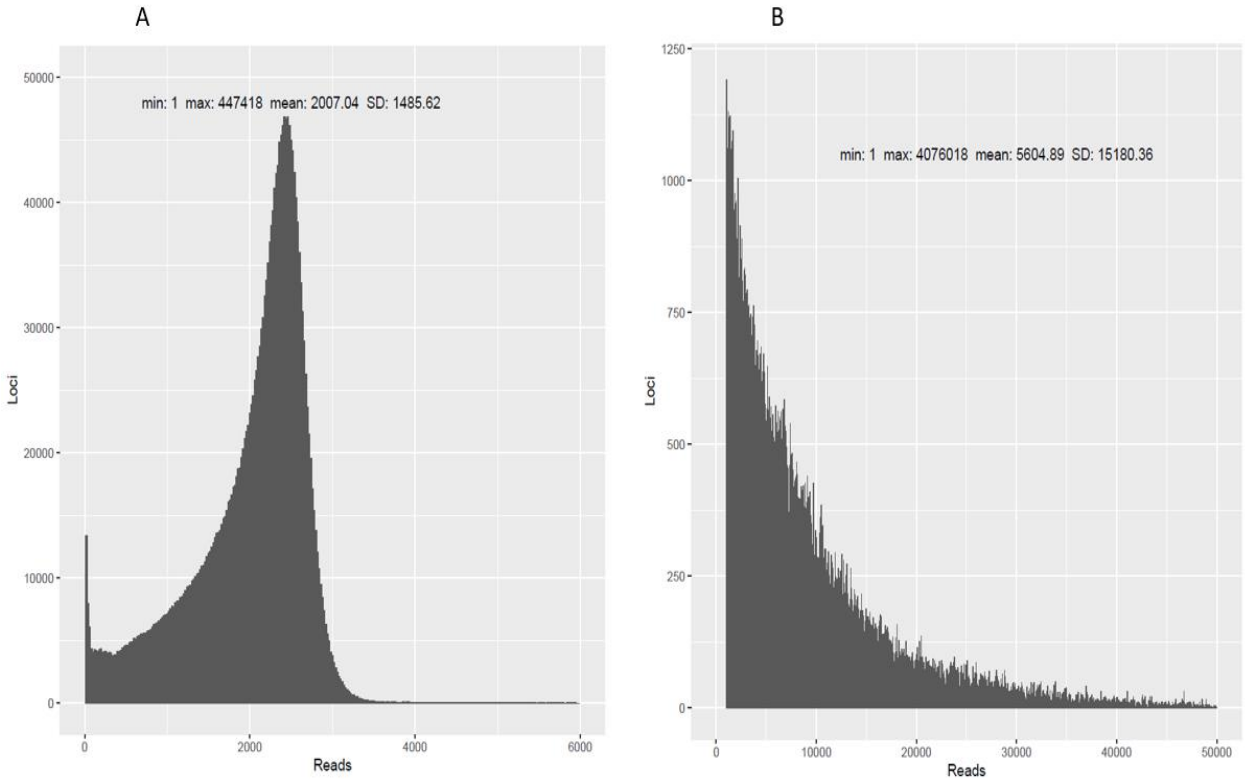

Figure S2. Distribution and summary statistics of the number of reads across unfiltered loci. (A) 276 fully sequenced samples from 47 colonies sampled in Betzet beach in northern Israel. (B) 47 RAD-sequenced samples of 47 colonies from which the fully sequenced samples also originate.

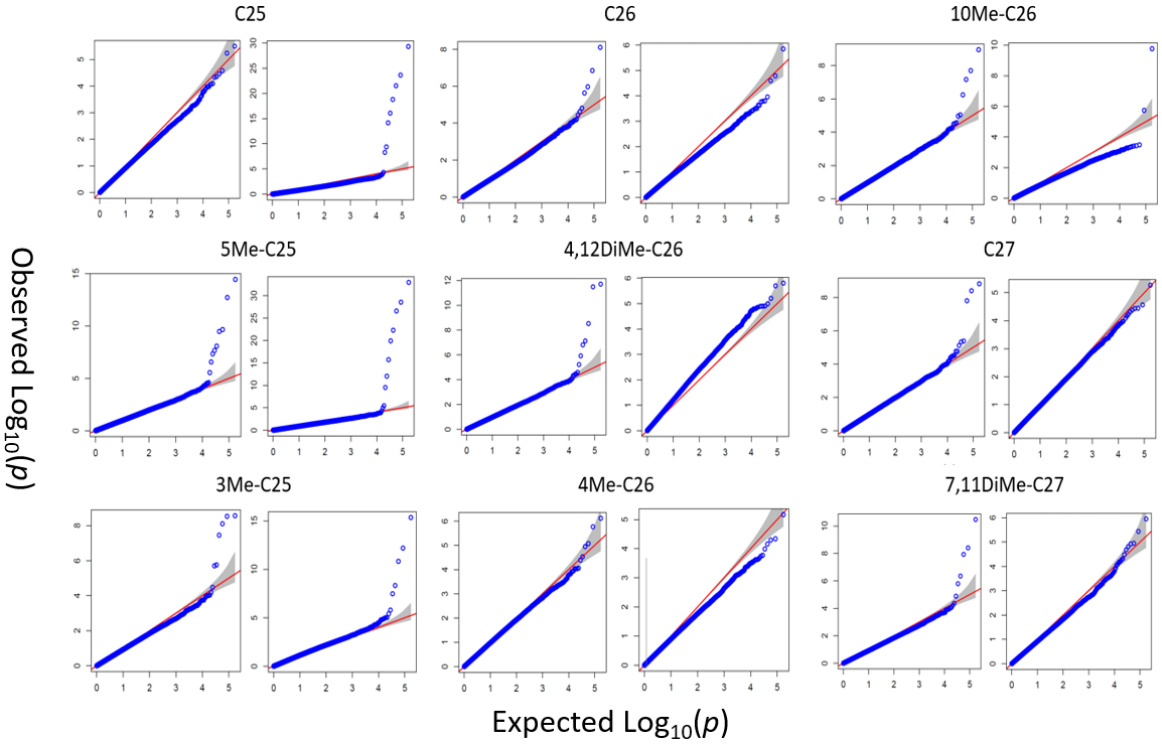

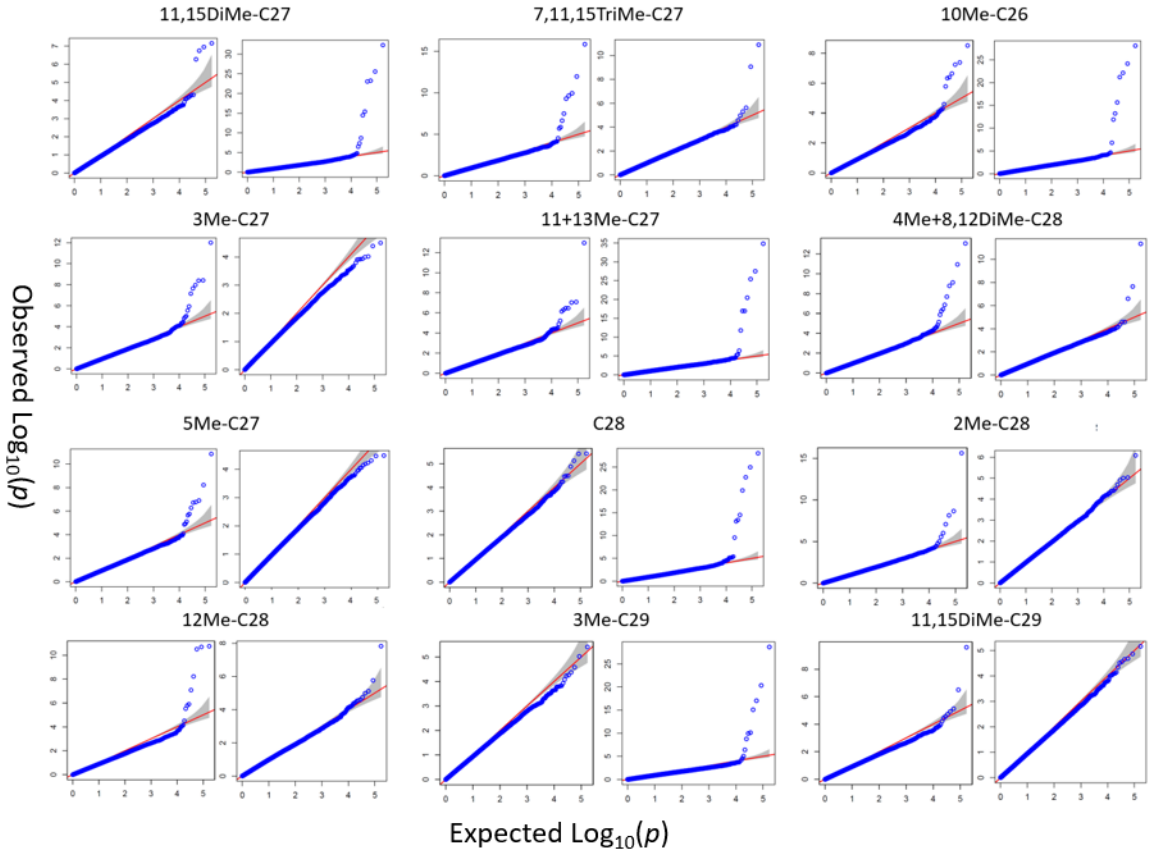
11,15DiMe-C27
7,11,15TriMe-C27
10Me-C26
3Me-C27
11+13Me-C27
4Me+8,12DiMe-C28
5Me-C27
C28
2Me-C28
12Me-C28
3Me-C29
11,15DiMe-C29
Observed Log10(p)
Expected Log10(p)

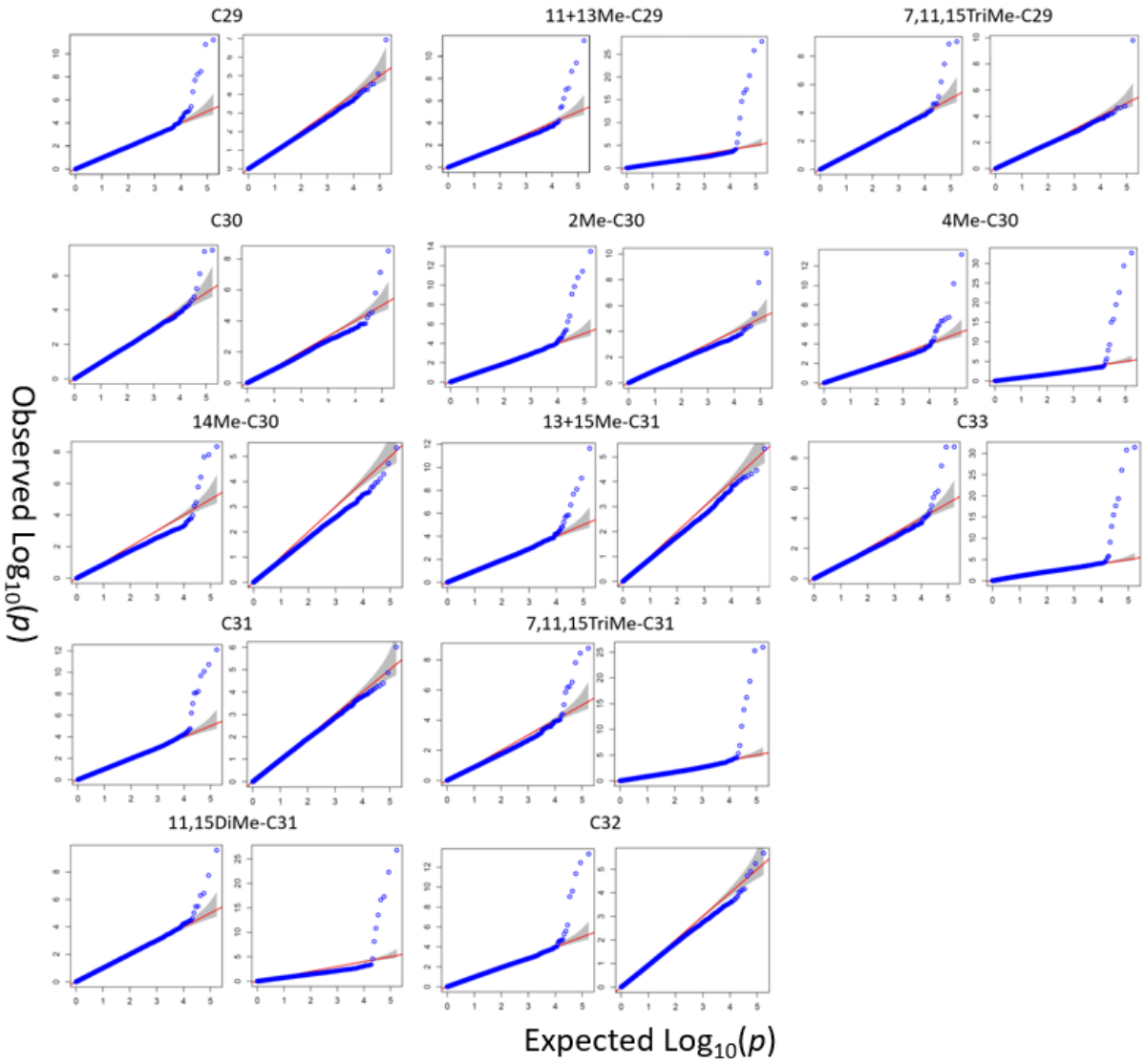

Figure S3. The assesment of how well the model used in the inidivual-level (left) and colony-level (right) analyses accounts for familial relatedness and population strcture for each of the CHC traits. The negative logarithms of the loci *p*-values S are plotted against their expected value under the null hypothesis of no association with the trait.

Table S1. Outlayer removals and normalization methods of the phenotype on the individual- and colony-levels.

Trait	Individuals outlayers	Individuals normalization	Colonies outlayers	Colonies normalization
C25	17	Yeo-Johnson	0	Log_b(x + a)
5Me-C25	44	Order norm	9	Log_b(x + a)
3Me-C25	22	Log_b(x + a)	4	Box Cox
C26	23	sqrt(x + a)	2	Box Cox
10Me-C26	13	Log_b(x + a)	2	sqrt(x + a)
4Me-C26	20	Order norm	3	Log_b(x + a)

4,12DiMe-C26	12	asinh(x)	1	sqrt(x + a)
C27	11	Order norm	2	Log_b(x + a)
5Me-C257	5	asinh(x)	0	sqrt(x + a)
11+13Me-C27	13	Order norm	2	Log_b(x + a)
11,15DiMe-C27	37	Order norm	9	Log_b(x + a)
7,11DiMe-C27	2	Yeo-Johnson	0	asinh(x)
3Me-C27	16	Box Cox	1	Box Cox
7,11,15TriMe-C27	21	exp(x)	4	asinh(x)
C28	37	Order norm	4	sqrt(x + a)
12Me-C28	13	Order norm	0	asinh(x)
4,12DiMe-C28	1	Box Cox	0	sqrt(x + a)
4Me+8,12DiMe-C28	16	sqrt(x + a)	0	Box Cox
2Me-C28	23	Order norm	2	sqrt(x + a)
C29	14	Box Cox	1	sqrt(x + a)
11+13Me-C29	13	Box Cox	1	Box Cox
11,15DiMe-C29	17	Yeo-Johnson	2	Log_b(x + a)
3Me-C29	34	Order norm	3	sqrt(x + a)
7,11,15TriMe-C29	5	Box Cox	3	sqrt(x + a)
C30	26	Yeo-Johnson	4	asinh(x)
14Me-C30	15	Box Cox	2	asinh(x)
4Me-C30	16	Order norm	0	Log_b(x + a)
2Me-C30	14	asinh(x)	4	Log_b(x + a)
C31	14	Log_b(x + a)	3	Box Cox
13+15Me-C31	11	exp(x)	4	sqrt(x + a)
11,15DiMe-C31	11	Box Cox	0	Log_b(x + a)
7,11,15TriMe-C31	4	Box Cox	0	asinh(x)
C32	13	asinh(x)	4	asinh(x)
C33	8	asinh(x)	0	sqrt(x + a)

Table S2. The mapping of significant loci (*q*-value < 0.3) on the genome. Individual-level results are in blue and colony-level results are in black**.** Loci that are mapped to the same or close genetic position (within 12cM) are marked with yellow or orange backgrounds. Both genetic and physical positioning are shown.

Chr	Genetic.pos	Scaffold	Position	CHC	q-value
1	0	scaffold17|size760598	515848	4,12DiMe-C26	0.279715055
1	2.87	scaffold35|size591243	473891	4,12DiMe-C26	0.11352072
1	9.66	scaffold296|size210905	44019	4,12DiMe-C26	0.279715055
1	34.15	scaffold578|size105271	38187	7,11,15TriMe-C27	0.168010666

1	88.15	scaffold916|size58012	4774	C31	0.118061549
1	88.15	scaffold293|size211391	198932	C33	0.281531387
2	65.4	scaffold636|size94593	82725	3Me-C25	0.281531387
3	85.67	scaffold320|size199217	33276	11+13Me-C27	0.259138689
3	87.52	scaffold1113|size42492	15042	4Me+8,12DiMe-C28	0.168010666
4	1.88	scaffold1163|size40329	39019	4Me+8,12DiMe-C28	0.201612799
4	16.6	scaffold558|size111151	58293	11+13Me-C29	0.145481369
4	39.56	scaffold77|size466230	39015	4,12DiMe-C26	0.23006866
4	39.56	scaffold551|size113931	79453	C31	0.144009142
4	83.57	scaffold326|size196711	73375	11+13Me-C27	0.009092586
4	143.72	scaffold220|size265453	70637	C32	0.163469837
4	181.71	scaffold734|size79827	17289	7,11,15TriMe-C27	0.23793943
4	203.11	scaffold74|size472645	164044	C31	0.118061549
5	131.68	scaffold35|size591243	43412	5Me-C25	0.106385132
6	70.38	scaffold336|size190304	25911	C29m3	0.181851711
6	90.66	scaffold737|size79726	15861	C28	0.251561534
7	52.75	scaffold107|size407829	186705	C33	0.281531387
7	56.43	scaffold859|size63718	3120	7,11,15TriMe-C27	0.168010666
7	57.35	scaffold19|size722566	429439	C31	0.144009142
7	62.08	scaffold279|size219011	173386	11,15DiMe-C27	0.018185171
7	101.52	scaffold30|size631625	144566	C28	0.275375449
7	104.36	scaffold85|size450463	361438	11+13Me-C29	0.175789988
7	111.1	scaffold28|size641708	145558	4Me+8,12DiMe-C28	0.21114854
7	135.68	scaffold404|size159223	63505	3Me-C25	0.281531387
8	126.41	scaffold194|size285062	81296	11+13Me-C29	0.175789988
8	137.97	scaffold618|size98603	6938	C31	0.118061549

8	208.22	scaffold658|size91109	44118	11,15DiMe-C27	0.297782177
8	222.43	scaffold740|size79674	67018	C32	0.096871015
8	259.2	scaffold20|size721085	484650	C29	0.28516405
8	309.3	scaffold751|size78167	6597	7,11,15TriMe-C29	0.287585825
9	45.61	scaffold54|size511285	140799	5Me-C25	0.009092586
9	85.74	scaffold235|size251712	52728	C32	0.090816576
9	119.36	scaffold219|size265940	180069	7,11,15TriMe-C27	0.168010666
9	137.13	scaffold311|size203550	120617	C29	0.186173981
9	142.85	scaffold505|size124814	43537	12Me-C28	0.093843796
9	142.85	scaffold66|size491290	166504	4Me+8,12DiMe-C28	0.276082392
10	105.07	scaffold306|size205911	65549	12Me-C28	0.093843796
10	132.88	scaffold75|size469975	364802	4Me+8,12DiMe-C28	0.21114854
11	2.02	scaffold146|size337763	226678	7,11,15TriMe-C27	0.271314522
11	17.44	scaffold291|size213446	9721	4Me-C30	0.099898234
11	44.83	scaffold22|size714790	90604	11+13Me-C27	0.275808429
11	111.65	scaffold67|size489733	28054	C31	0.189579603
11	153.29	scaffold622|size97615	36744	3Me-C25	0.292883459
11	312.17	scaffold508|size123518	117137	12Me-C28	0.093843796
12	0	scaffold730|size80008	50311	2Me-C30	0.240663927
12	67.25	scaffold71|size482159	21063	4Me+8,12DiMe-C28	0.21114854
12	77.84	scaffold71|size482159	252805	4Me+8,12DiMe-C28	0.215941637
12	87.97	scaffold593|size103847	95748	11+13Me-C29	0.19614006
12	94.99	scaffold65|size491780	101529	7,11,15TriMe-C27	0.271314522
12	115.45	scaffold209|size272198	146941	5Me-C25	0.045408288
12	141.58	scaffold470|size137511	24197	C31	0.226032368
14	40.37	scaffold44|size549762	519588	11+13Me-C29	0.175789988
14	48.21	scaffold581|size104792	64268	5Me-C25	0.207830527

14	50.17	scaffold125|size365959	224995	7,11,15TriMe-C29	0.254286414
14	92.55	scaffold204|size276989	165280	4Me+8,12DiMe-C28	0.072653261
14	95.38	scaffold144|size340398	186437	5Me-C25	0.141844335
14	107.79	scaffold3|size1157121	1010964	2Me-C30	0.265638486
14	127.94	scaffold130|size360227	149410	4Me+8,12DiMe-C28	0.168010666
15	52.68	scaffold72|size474807	247511	4,12DiMe-C26	0.11352072
15	90.15	scaffold124|size367063	14584	5Me-C25	0.093086991
15	94.21	scaffold99|size421651	410341	5Me-C25	0.027244973
15	174.71	scaffold212|size271006	160026	11+13Me-C27	0.172551495
16	40.47	scaffold1|size1555347	1092532	11,15DiMe-C27	0.297782177
17	55.6	scaffold299|size209978	118401	C31	0.118061549
17	68.45	scaffold29|size639771	423039	5Me-C25	0.072740685
17	147.15	scaffold608|size100611	57366	7,11,15TriMe-C27	0.018163315
18	74.77	scaffold153|size330014	258009	12Me-C28	0.220230198
18	117.35	scaffold61|size494520	99800	11+13Me-C29	0.175789988
18	136.63	scaffold13|size775888	175137	5Me-C25	0.141844335
18	148.94	scaffold74|size472645	467205	C28	0.227314639
20	0	scaffold1423|size26545	12315	5Me-C25	0.181851711
20	83.75	scaffold53|size513719	234805	4Me+8,12DiMe-C28	0.108979892
20	110.88	scaffold392|size162570	49495	5Me-C25	0.045462928
21	56.5	scaffold52|size514423	369128	7,11,15TriMe-C29	0.254286414
22	85.98	scaffold271|size223719	127531	C28	0.24549981
23	19.07	scaffold16|size761867	381681	3Me-C25	0.281531387
23	45.16	scaffold180|size296944	252701	C29	0.28516405
23	252.96	scaffold588|size104489	7055	C29	0.28516405
23	278.7	scaffold583|size104635	55219	C28	0.275375449
23	346.55	scaffold27|size651064	287045	C32	0.174367827

23	347.46	scaffold113|size393933	273321	2Me-C30	0.118061549
23	370.92	scaffold232|size254158	2527	5Me-C25	0.106385132
24	143.62	scaffold323|size197691	182834	2Me-C30	0.265638486
24	189.98	scaffold628|size95885	66061	C29	0.186173981
24	243.79	scaffold215|size268708	257542	11+13Me-C29	0.232997505
24	284.75	scaffold26|size661983	198368	5Me-C25	0.106385132
25	67.31	scaffold6|size960371	700278	C32	0.090816576
25	84.71	scaffold155|size327501	273726	C31	0.144009142
25	94.57	scaffold19|size722566	309358	C28	0.261411835
26	21.23	scaffold553|size113576	90729	11,15DiMe-C27	0.297782177
26	33.21	scaffold33|size606826	197846	12Me-C28	0.292429376
26	127.17	scaffold804|size70630	40423	5Me-C25	0.093086991
26	221.23	scaffold57|size507111	381549	C28	0.275375449
26	278.97	scaffold303|size207491	10542	11+13Me-C29	0.145481369
26	309.97	scaffold8|size894206	191498	7,11,15TriMe-C27	0.264881681